MADRID
inter.noise 2019
June 16 - 19

NOISE CONTROL FOR A BETTER ENVIRONMENT

Modal Damping Estimation for Structure-Borne Sound Predictions Using an Extended Modal Strain and Kinetic Energy Method

Takebayashi, Kenichi[1] and Tanaka, Aya[2]
Kajima Technical Research Institute
2-19-1 Tobitakyu, Chofu, Tokyo, Japan

Andow, Kei[3]
Andow Environmental Consultant
2-5-15, Kami-ishiwara, Chofu, Tokyo, Japan

Yamaguchi, Takao[4]
Faculty of Science and Technology, Gunma University
1-5-1 Tenjin-cho, Kiryu, Gunma, Japan

ABSTRACT

A practical method for predicting vibration and structure-borne sound in buildings is developed using an extended Modal Strain and Kinetic Energy (MSKE) method. The proposed method introduces a complex Young's Modulus for structural materials, a complex bulk modulus and an effective density for the acoustical fluid in order to express damping behaviour of the system. This method allows for the modal loss factor to be obtained without solving complex eigenvalue problems under the assumption that the complex eigenvector can be approximated by the real eigenvector. Under the given assumptions, the proposed method reduces complexity and computational requirements compared to the traditional MSKE method by solving for the scalar pressure rather than the vector quantity displacement. The proposed method was experimentally validated in a two-story structure made of reinforced concrete. The second floor slab was excited by an impact hammer while the driving point acceleration and sound pressure were measured in the room below. The building frame and cavity were modeled and discretized by a five centimeter rectangular mesh. Accelerance and the sound transfer function were calculated and compared to the measured results. In the low-frequency region (up to 150 Hz), both calculated results agreed well with the measured results.

---

[1] takebayk@kajima.com
[2] tanakaay@kajima.com
[3] kei@andow-k.com
[4] yamagum3@gunma-u.ac.jp

1. INTRODUCTION

To control noise, vibration and structure-borne sound in buildings, accurate prediction methods are necessary. Some numerical methods, such as the Finite Element Method (FEM) is one such accurate prediction method. Modal analysis theory based on solving generalized eigenvalue problems on a finite element matrix is widely used for determining the vibration characteristics (mode shapes and natural frequencies) of the building structure. To calculate the frequency response using modal analysis theory, the modal loss factor of the system has to be determined. For the structural system, comprised of various material components, the Modal Strain Energy (MSE) method was proposed [3] to estimate the modal loss factor. The MSE method introduces a complex Young's modulus for the structural materials in order to express the structure's damping behavior. By the MSE method, approximated values of the modal loss factor at each mode are calculated by means of real eigenvectors obtained by solving real eigenvalue problems under the assumption that the complex eigenvector can be approximated by the real eigenvector. For structural-acoustic coupling problems which take acoustic radiation into consideration, such as floor impact sound or structure-borne sound generated by a building's mechanical equipment, the Modal Strain and Kinetic Energy (MSKE) method has been proposed [4] to estimate the modal loss factors. In the MSKE method, particle displacement is used as a nodal unknown variable of the finite elements in the acoustical region. Acoustical and structural components at the boundary between the acoustical and structural regions can be connected directly, because displacement is a common nodal unknown variable for the structural-acoustical coupling system. Although using displacements as common unknowns helps us to construct an FE matrix of the coupling system, as displacements are vector quantities, memory consumption will increase rapidly as the acoustical region increases in size.

In this paper, we propose an extended MSKE method for solving structural-acoustic coupling systems using sound pressure as the FEM nodal unknowns in the acoustical region. The proposed method, including how to calculate the modal loss factor, are briefly described along with the experimental validation results.

2. Theory

2.1 Structural-acoustic coupling system

Considering a general impact source on a structure with FEM, the equations of motion for the un-damped structural-acoustic coupling system are given by:

$$\left(\begin{bmatrix} K_{ss} & K_{sa} \\ 0 & K_{aa} \end{bmatrix} - \omega^2 \begin{bmatrix} M_{ss} & 0 \\ M_{as} & M_{aa} \end{bmatrix} \right) \begin{Bmatrix} u \\ p \end{Bmatrix} = \begin{Bmatrix} f_s \\ 0 \end{Bmatrix}, \tag{1}$$

where, K_{ss} and K_{aa} are the stiffness matrices in the structural and acoustical region, and M_{ss} and M_{aa} are the mass matrices in the structural and acoustical region respectively. u is a nodal displacement vector of the structural component in meters, p is a nodal sound pressure vector of the acoustical components in pascals, f_s is a nodal force vector applied to the structural region in newtons, and ω is the angular frequency in radians per second.

The coupling terms K_{sa} and M_{as} have the following relation:

$$K_{sa} = -M_{as}^t, \tag{2}$$

where the subscripts s and a indicate variables in the structural or acoustical regions respectively. The superscript t indicates the transpose of the matrix.

Although the frequency response of this system can be obtained by solving a linear equation at each frequency, the computational time can be quite lengthy if there are a large number of frequencies to be solved. Moreover, if the excitation point is changed, all the calculations must be repeated. On the other hand, by using modal analysis to obtain the frequency response, the eigenvalue problem needs only be solved once. Once eigenvalues and eigenvectors are obtained, the frequency response of the structural system can be calculated using less computational time compared to solving a linear equation of the system at various individual frequencies. The right-eigenvector, obtained by solving the right-eigenvalue problem of Equation 1 (x in $Ax = \lambda x$), cannot diagonalize stiffness and mass matrices, thus the modal analysis cannot be applied to structural-acoustic coupling systems when only using the right-eigenvector.

2.2 Left and Right Eigenvector

Hagiwara [1] introduced the left-eigenvector (y in $y^t A = \lambda y^t$) to form the diagonalizable asymmetric matrices of Equation 1. Jianhui [2] derived the left-eigenvector when Component Mode Synthesis (CMS) is applied to Equation 1. If $[W_s^t \quad W_a^t]^t$ is the left-eigenvector matrix, and $[D^t V_s^t \quad V_a^t]^t$ is the right-eigenvector matrix, the relation between the left and right-eigenvector is:

$$\begin{bmatrix} W_s \\ W_a \end{bmatrix} = \begin{bmatrix} V_s D \\ V_a \end{bmatrix}, \tag{3}$$

where

$$[D] = \mathrm{diag}\{\lambda^{(1)}, \lambda^{(2)}, \cdots, \lambda^{(M)}\}, \tag{4}$$

$$[V_s] = \left[\phi_s^{(1)}, \phi_s^{(2)}, \cdots, \phi_s^{(M)}\right] \quad , \quad [V_a] = \left[\phi_a^{(1)}, \phi_a^{(2)}, \cdots, \phi_a^{(M)}\right], \tag{5), (6}$$

$$[W_s] = \left[\psi_s^{(1)}, \psi_s^{(2)}, \cdots, \psi_s^{(M)}\right] \quad , \quad [W_a] = \left[\psi_a^{(1)}, \psi_a^{(2)}, \cdots, \psi_a^{(M)}\right], \tag{7), (8}$$

$\lambda^{(i)}$ is the ith eigenvalue, M is the number of modes, and $\phi_s^{(i)}$, $\phi_a^{(i)}$, $\psi_s^{(s)}$ and $\psi_a^{(s)}$ are the ith right and left-eigenvector corresponding to the structural and acoustical regions respectively. Using the left-eigenvector in Equation 3, the stiffness and mass matrices of Equation 1 can become diagonalizable and modal analysis theory can be applied.

2.3 Frequency Response

According to modal analysis theory, the frequency response of the system can be calculated by Equation 9 below.

$$x_r(\omega) \text{ or } p_r(\omega) = \sum_{i=1}^{M} \frac{\phi_r^{(i)} \psi_q^{(i)}}{\lambda^{(i)} - \omega^2 + j\lambda^{(i)} \varepsilon^{(i)}} f(\omega), \tag{9}$$

where, $x_r(\omega)$ and $p_r(\omega)$ are the displacement and sound pressure at degree of freedom r obtained when the degree of freedom q is excited by the force $f(\omega)$, in newtons, at an angular frequency ω in radians per second. Integer i represents modal order, $\phi_r^{(i)}$ is the ith right-eigenvector at degree of freedom r, $\psi_q^{(i)}$ is the ith left-eigenvector at degree of freedom q, $\lambda^{(i)}$ is i^{th} eigenvalue, $\varepsilon^{(i)}$ is i^{th} modal loss factor of the system and j is the

imaginary unit ($\sqrt{-1}$). As shown in Equation 9, to calculate the frequency response of the system, the modal damping has to first be determined.

2.3 Extended Modal Strain and Kinetic Energy Method

In this section, the extended MSKE method to determine the modal loss factor for the structural-acoustic coupling system, using sound pressure as the nodal unknowns in the acoustic region, is briefly described. To take material damping into account, the Young's modulus E of the structural material, bulk modulus κ, and density ρ of the acoustical fluid are changed to a complex quantity with their material loss factors determined as below:

$$\hat{E} \equiv E_R + jE_I = E_R\left(1 + j\frac{E_I}{E_R}\right) = E_R(1 + j\eta_s) \quad \text{where,} \quad \eta_s = E_I/E_R, \qquad (10), (11)$$

$$\hat{\kappa} \equiv \kappa_R + j\kappa_I = \kappa_R\left(1 + j\frac{\kappa_I}{\kappa_R}\right) = \kappa_R(1 + j\eta_a) \quad \text{where,} \quad \eta_a = \kappa_I/\kappa_R, \qquad (12), (13)$$

$$\hat{\rho} \equiv \rho_R + j\rho_I = \rho_R\left(1 + j\frac{\rho_I}{\rho_R}\right) = \rho_R(1 + j\chi_a) \quad \text{where,} \quad \chi_a = \rho_I/\rho_R, \qquad (14), (15)$$

The subscript R and I indicate the real and imaginary parts of the complex quantity and the hat symbol denotes a complex quantity. η_s represents the material loss factor of the structural component, η_a and χ_a are the loss factors of the acoustic fluid. The damping factor η_a and χ_a can be calculated from the characteristic impedance and sound propagation constant of the acoustic fluid [5]. If the acoustic region is filled with air, these damping factors η_a and χ_a are small. The stiffness and mass matrices are also changed to complex quantities as below:

$$[\hat{K}_{ss}] \equiv [K_{ss}](1 + j\eta_s), \qquad (16)$$

$$[\hat{K}_{aa}] \equiv \frac{1}{1+j\chi_a}[K_{aa}] = \frac{1}{1+\chi_a^2}[K_{aa}](1 - j\chi_a), \qquad (17)$$

$$[\hat{M}_{aa}] \equiv \frac{1}{1+j\eta_a}[M_{aa}] = \frac{1}{1+\eta_a^2}[M_{aa}](1 - j\eta_a), \qquad (18)$$

The generalized right-eigenvalue problem (matrix form) is represented in Equation 19.

$$\begin{bmatrix} \hat{K}_{ss} & K_{sa} \\ 0 & \hat{K}_{aa} \end{bmatrix} \begin{bmatrix} \hat{V}_s \\ \hat{V}_a \end{bmatrix} = \begin{bmatrix} M_{ss} & 0 \\ M_{as} & \hat{M}_{aa} \end{bmatrix} \begin{bmatrix} \hat{V}_s \\ \hat{V}_a \end{bmatrix} [\hat{D}]. \qquad (19)$$

The eigenvalue and left and right eigenvector also become complex quantities.

$$\hat{\lambda}^{(i)} \equiv \lambda^{(i)}\left(1 + j\eta^{(i)}\right), \qquad (20)$$

$$\hat{\phi}^{(i)} \equiv \phi_R^{(i)} + j\phi_I^{(i)} \quad , \quad \hat{\psi}^{(i)} \equiv \psi_R^{(i)} + j\psi_I^{(i)}. \qquad (21), (22)$$

The Rayleigh quotient of the ith mode is represented in Equation 23.

$$\hat{\lambda}^{(i)} = \begin{Bmatrix} \hat{\psi}_s^{(i)} \\ \hat{\psi}_a^{(i)} \end{Bmatrix}^t \begin{bmatrix} \hat{K}_{ss} & K_{sa} \\ 0 & \hat{K}_{aa} \end{bmatrix} \begin{Bmatrix} \hat{\phi}_s^{(i)} \\ \hat{\phi}_a^{(i)} \end{Bmatrix} \Bigg/ \begin{Bmatrix} \hat{\psi}_s^{(i)} \\ \hat{\psi}_a^{(i)} \end{Bmatrix}^t \begin{bmatrix} M_{ss} & 0 \\ M_{as} & \hat{M}_{aa} \end{bmatrix} \begin{Bmatrix} \hat{\phi}_s^{(i)} \\ \hat{\phi}_a^{(i)} \end{Bmatrix}. \tag{23}$$

Here, we introduce the assumption that the complex left and right eigenvector can be approximated by real left and right eigenvectors obtained by solving real eigenvalue problems, i.e.,

$$\hat{\psi}^{(i)} \approx \psi^{(i)} \quad , \quad \hat{\phi}^{(i)} \approx \phi^{(i)} \tag{24}, (25)$$

The Rayleigh quotient is developed using Equations 16 through 18, which results in

$$\lambda^{(i)}\left(1 + j\varepsilon^{(i)}\right) \quad \approx \quad \frac{k^{(i)} - \chi_a^2 \bar{k}_{aa}^{(i)} + j\left(\eta_s k_{ss}^{(i)} - \chi_a \bar{k}_{aa}^{(i)}\right)}{m^{(i)} - j\eta_a^2\,\bar{m}_{aa}^{(i)} - j\eta_a\,\bar{m}_{aa}^{(i)}}, \tag{26}$$

where

$$k_{ss}^{(i)} = \left\{\psi_s^{(i)}\right\}^t [K_{ss}]\left\{\phi_s^{(i)}\right\} \quad , \quad m_{ss}^{(i)} = \left\{\psi_s^{(i)}\right\}^t [M_{ss}]\left\{\phi_s^{(i)}\right\}, \tag{27}, (28)$$

$$k_{sa}^{(i)} = \left\{\psi_s^{(i)}\right\}^t [K_{sa}]\left\{\phi_a^{(i)}\right\} \quad , \quad m_{as}^{(i)} = \left\{\psi_a^{(i)}\right\}^t [M_{as}]\left\{\phi_s^{(i)}\right\}, \tag{29}, (30)$$

$$k_{aa}^{(i)} = \left\{\psi_a^{(i)}\right\}^t [K_{aa}]\left\{\phi_a^{(i)}\right\} \quad , \quad m_{aa}^{(i)} = \left\{\psi_a^{(i)}\right\}^t [M_{aa}]\left\{\phi_a^{(i)}\right\}, \tag{31}, (32)$$

$$k^{(i)} = k_{ss}^{(i)} + k_{sa}^{(i)} + k_{aa}^{(i)} \quad , \quad m^{(i)} = m_{ss}^{(i)} + m_{as}^{(i)} + m_{aa}^{(i)}, \tag{33}, (34)$$

$$\frac{1}{1+\chi_a^2} k_{aa}^{(i)} = \bar{k}_{aa}^{(i)} \quad , \quad \frac{1}{1+\eta_a^2} m_{aa}^{(i)} = \bar{m}_{aa}^{(i)}. \tag{35}, (36)$$

$k^{(i)}$ and $m^{(i)}$ represent the ith modal stiffness and modal mass respectively. Finally, the ith eigenvalue and modal loss factor are obtained by the following equations.

$$\lambda^{(i)} = \frac{k^{(i)}}{m^{(i)}} \cdot \frac{1 - \left(\eta_s S_s^{(i)} - \chi_a S_a^{(i)}\right)\eta_a R_a^{(i)} - \eta_a^2 R_a^{(i)} - \chi_a^2 S_a^{(i)} + \eta_a^2 R_a^{(i)} \chi_a^2 S_a^{(i)}}{\left(1 - \eta_a^2 R_a^{(i)}\right)^2 + \left(\eta_a R_a^{(i)}\right)^2}, \tag{37}$$

$$\varepsilon^{(i)} = \frac{\eta_a R_a^{(i)} + \left(\eta_s S_s^{(i)} - \chi_a S_a^{(i)}\right) + \chi_a^2 S_a^{(i)} \eta_a R_a^{(i)} + \left(\eta_s S_s^{(i)} - \chi_a R_a^{(i)}\right)\eta_a^2 R_a^{(i)}}{1 - \left(\eta_s S_s^{(i)} - \chi_a S_a^{(i)}\right)\eta_a R_a^{(i)} - \eta_a^2 R_a^{(i)} - \chi_a^2 S_a^{(i)} + \eta_a^2 R_a^{(i)} \chi_a^2 S_a^{(i)}}, \tag{38}$$

$$S_s^{(i)} = \frac{k_{ss}^{(i)}}{k^{(i)}} \quad , \quad S_a^{(i)} = \frac{\bar{k}_{aa}^{(i)}}{k^{(i)}} \quad , \quad R_a^{(i)} = \frac{\bar{m}_{aa}^{(i)}}{m^{(i)}}. \tag{39}, (40), (41)$$

Equations 39 and 40 show the contribution ratios of structural and acoustical components to the ith modal stiffness values. Equation 41 also represents the contribution ratio of the acoustical component to the ith modal mass. In Equation 37, the term $k^{(i)}/m^{(i)}$ corresponds to the eigenvalue obtained by the real eigenvalue problem. Therefore, the eigenvalue calculated by Equation 37 becomes a slightly small value

compared to the real eigenvalue. By considering $S_{\text{s}}^{(i)}$, $S_{\text{a}}^{(i)}$ and $R_{\text{a}}^{(i)}$ take values between zero to one and η_s, η_a and $\chi_a \ll 1$, their product and squared values ($\eta_s\eta_a$, $\eta_a\chi_a$, η_s^2, η_a^2, χ_a^2) can be considered negligible. Therefore, the ith eigenvalue and modal loss factor can be simplified to:

$$\lambda^{(i)} \approx \frac{k^{(i)}}{m^{(i)}}, \tag{42}$$

$$\varepsilon^{(i)} \approx \eta_k^{(i)} + \eta_m^{(i)}, \tag{43}$$

where

$$\eta_k^{(i)} = \eta_{\text{s}}S_{\text{s}}^{(i)} - \chi_{\text{a}}S_{\text{a}}^{(i)} \quad , \quad \eta_m^{(i)} = \eta_{\text{a}}R_{\text{a}}^{(i)}. \tag{44), (45}$$

The subscripts k and m indicate stiffness and mass. Equation 42 implies that if the material loss factor is small, eigenvalues are not changed to the real eigenvalue ($k^{(i)}/m^{(i)}$). Equation 43 implies that the modal loss factor can be obtained from the same form as the conventional MSKE method [4]. In this paper, we use the Equation 42 and 43 to calculate the frequency response.

3. Experimental Validation

3.1 Structural Frame

The proposed method was experimentally validated. The experiment was carried out on a two-story reinforced concrete frame structure. Plan and section views are shown in Fig. 1. Excitation point on the second floor and receiver point in Room 1 are also shown. For the numerical simulation, the building was discretized by a 5 cm rectangular mesh. Note that only the magenta color walls and slabs shown in Figure 1 and 2 are modeled. The degrees of freedom for the structural region was 605,967 and the acoustical region was 499,041. The material parameter used in the calculation is shown in Table 1. Component Mode Synthesis [2] was applied to solve the eigenvalue problem given in Equation 1. The number of eigenvalues and eigenvectors for the structural region was 128 and the acoustical region was 998. The frequency response between 10 - 500 Hz was calculated using Equation 9. The sound pressure in Room 1 was measured and calculated when the second floor concrete slab was excited by an impact hammer. Driving point acceleration was also measured and calculated. In this paper, all calculations were implemented using MATLAB R2017b.
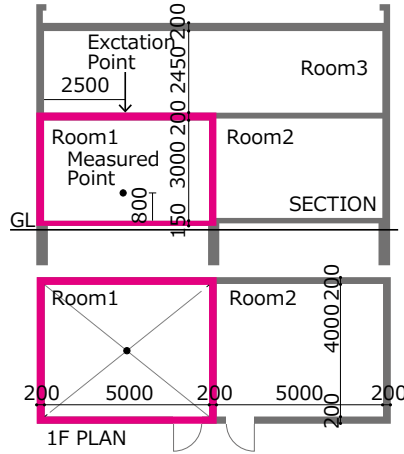
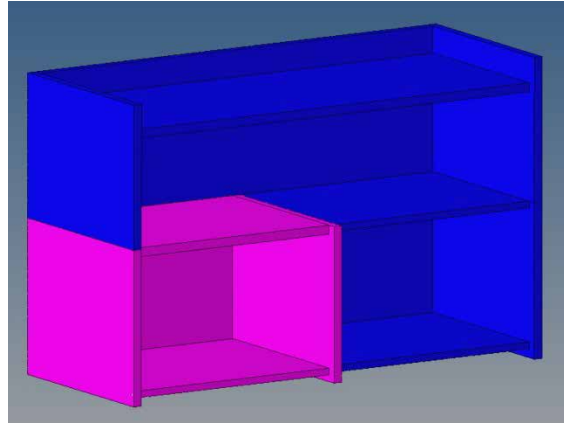*Fig. 1 Wall type frame structure. Section (Above) and plan (Bottom) views.*

Fig. 2 3D model used to carry out calculation

Table 1. *Material properties used in the calculation*

Material	E / κ **[Pa]**	ρ **[kg/m³]**	ν **[-]**	η **[-]**	χ **[-]**
Reinforced concrete	3.2E10	2400	0.17	0.02	-
Air	1.4E5	1.2	-	0.001	−0.001

3.2 Comparison between measured and calculated results

3.2.1 Accelerance on the slab

The measured and calculated driving point accelerance is shown in Figure 3. Up to 150 Hz, both results appear to reasonably agree, but above 150 Hz, peak amplitude at resonance frequencies varies between the measured and calculated results. Since peak amplitude is determined by the modal loss factor, the estimated modal loss factor is lower than the actual value. In principle, the upper bound of the modal loss factor obtained by the MSKE method corresponds to a maximum material loss factor used in the calculation. Therefore, another damping factor appears to contribute to the material loss factor in this case.

3.2.2   Sound pressure in Room 1

The measured and calculated transfer function of the sound pressure in pascals per newton is shown in Figure 4. Up to 200 Hz, the overall characteristics of the measured and calculated results agree fairly well, though the peak amplitude shows to be lower than the measured results. This discrepancy may be due to the loss factor of air. For further accuracy, the actual loss factor of air should be considered. Above 200 Hz, there are various peaks in the frequency response making it is difficult to trace each mode. 1/3 octave band averaged values are also shown in Figure 4, which show fair agreement above 200 Hz.
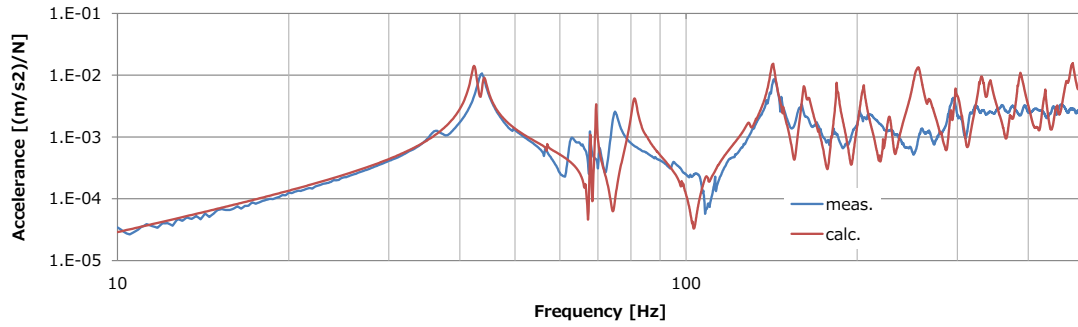
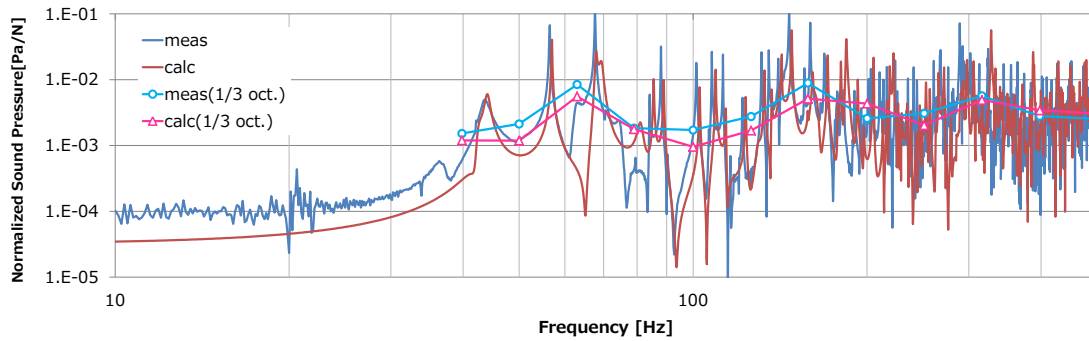Fig. 3 Driving point accelerance on the 2nd floor slab.

Fig. 4 Normalized Sound Pressure (sound pressure / force) in Room 1.

4. CONCLUSIONS

This paper proposed and described an extended MSKE method to solve a building structural-acoustic coupling system using sound pressure as nodal unknown variables in the acoustical region. Experimental validation was carried out in a two-story structure. The sound pressure in Room 1 was measured and calculated when the second floor concrete slab was excited by an impact hammer. Driving point acceleration was also measured and calculated. Comparing the measured and calculated results, overall frequency characteristics showed similarities below 150Hz. Above 150Hz, peak amplitudes, particularly acceleration results, showed fair differences. This discrepancy could be caused by the damping property of reinforced concrete. Further improvement is planned for focusing on the measurement of the damping properties for actual conditions.

6. REFERENCES

1. I. Hagiwara, Z. D. Ma, A. Arai and K. Nagabuchi, *"Reduction of Vehicle Interior Noise Using Structural-Acoustic Sensitivity Analysis Methods"*, SAE Transactions (1991), 100(6), 267-276.

2. Jianhui Luo and Hae Chang Gea, *"Modal Sensitivity Analysis of Coupled Acoustic-Structural Systems, Journal of Vibration and Acoustics"*, Journal of Vibration and Acoustics (1997), 119, 545–550.

3. Conor D. Johnson and David A. Kienholz, *"Finite Element Prediction of Damping in Structures with Constrained Viscoelastic Layers"*, AIAA Journal (1982), 20 (9), 1284–1290.

4. T. Yamaguchi, Y. Kurosawa, H. Enomoto, *"Damped vibration analysis using finite element method with approximated modal damping for automotive double walls with a porous material"*, Journal of Sound and Vibration (2009), 325, 436-450.

5. H. Utsuno, T. Tanaka, T. Fujikawa, *"Transfer Function Method for Measuring Characterisic Impedance and Propagation Constant of Porous materials"*, Journal of the Acoustical Society of America (1989), 86 (2) , 637-643